ADVANCES IN POLYMER SCIENCE 178

Polymeric and Inorganic Fibers

ringer

Polymeric and Inorganic Fibers

With contributions by
J. J. M. Baltussen · P. den Decker · T. Ishikawa · M. G. Northolt ·
S. J. Picken · R. Schlatmann

Springer

The series presents critical reviews of the present and future trends in polymer and biopolymer science including chemistry, physical chemistry, physics and material science. It is addressed to all scientists at universities and in industry who wish to keep abreast of advances in the topics covered.

As a rule, contributions are specially commissioned. The editors and publishers will, however, always be pleased to receive suggestions and supplementary information. Papers are accepted for "Advances in Polymer Science" in English.

In references Advances in Polymer Science is abbreviated *Adv Polym Sci* and is cited as a journal.

The electronic content of APS may be found springerlink.com

Library of Congress Control Number: 2004117780

ISSN 0065-3195
ISBN-10 3-540-24016-0 **Springer Berlin Heidelberg New York**
ISBN-13 978-3-540-24016-7 **Springer Berlin Heidelberg New York**
DOI 10.1007/b104206

Springer is a part of Springer Science+Business Media
springeronline.com

Printed in Germany

Cover design: KünkelLopka GmbH, Heidelberg/design & production GmbH, Heidelberg
Typesetting: Fotosatz-Service Köhler GmbH, Würzburg

Printed on acid-free paper 02/3141 xv – 5 4 3 2 1 0

Editorial Board

Advances in Polymer Science Also Available Electronically

For all customers who have a standing order to Advances in Polymer Science, we offer the electronic version via SpringerLink free of charge. Please contact your librarian who can receive a password for free access to the full articles by registering at:

springerlink.com

If you do not have a subscription, you can still view the tables of contents of the volumes and the abstract of each article by going to the SpringerLink Homepage, clicking on "Browse by Online Libraries", then "Chemical Sciences", and finally choose Advances in Polymer Science.

You will find information about the

- Editorial Board
- Aims and Scope
- Instructions for Authors
- Sample Contribution

at springeronline.com using the search function.

Contents

Adv Polym Sci (2005) 178: 1–108
DOI 10.1007/b104207

The Tensile Strength of Polymer Fibres

M. G. Northolt (✉) · P. den Decker · S. J. Picken · J. J. M. Baltussen · R. Schlatmann

[1] Magellan Systems International, 8310 Shell Road, Richmond VA 23237, USA
mafe.northolt@wxs.nl
[2] Teijin Twaron Research, P.O. Box 9600, 6800 TC Arnhem, The Netherlands
[3] Delft University of Technology, Polymer Materials & Engineering, Julianalaan 136, 2628 BL Delft, The Netherlands
s.j.picken@tnw.tudelft.nl
[4] Akzo Nobel Chemicals Research Arnhem, P.O. Box 9300, 6800 SB Arnhem, The Netherlands

Abstract A theory of the tensile strength of oriented polymer fibres is presented. From an analysis of the observed fracture envelope it is shown that the criterion for fracture of the fibre is either a critical shear stress or a critical shear strain. Owing to the chain orientation distribution in the fibre, the initiation of fracture is likely to occur in domains whose symmetry axes have orientation angles in the tail of this distribution. By considering the fibre as a molecular composite, the tensile strength is calculated as a function of the modulus. The results are compared to the observed values of PET, POK, cellulose II, PpPTA, PBO and PIPD fibres. In addition, the relation between the ultimate strength and the chain length distribution is investigated. By using the critical shear strain as a fracture criterion in the Eyring reduced time model, relations are derived for the fibre strength as a function of the load rate, as well as for the lifetime under constant load. Moreover, this model predicts the dependence of the strength on the temperature. The theoretical relations are compared to the experimental results on PpPTA fibres.

Keywords Polymer fibre · Strength · Chain length distribution · Creep fracture · Lifetime · Poly(*p*-phenylene terephthalamide)

Abbreviations and Symbols

A	Cross-sectional area
c	Concentration
d_c	Interplanar spacing
d.r.	Draw ratio
D	Diameter of the fibre
DABT	Poly(*p*-benzanilide terephthalamide)
DP	Degree of polymerisation
e_c	Chain modulus
e_l	Modulus transverse to the chain axis
esd	Estimated standard deviation
E	Fibre modulus
ERT	Eyring reduced time
$f(z)$	Chain length distribution
$f_w(z)$	Molecular weight distribution
g	Shear modulus of the domain
g_v	Apparent shear modulus
G	Torsional modulus of the filament

HT	High tenacity
h(z)	Crossing length distribution
I(U)	Transition density distribution
$j(t)$	Creep compliance
k_B	Boltzmann constant
K	Kelvin
L_d	Contour projection length of the chain
L_C	Contour length
L_G	Griffith crack length
L_P	Persistence length of the chain
m	Weibull modulus
M_n	Number-average molecular weight
M_w	Weight-average molecular weight
M_z	Z-average molecular weight
m.u.	Monomeric unit
N_A	Avogrado's number
p	Distance between periodic force centres
PAN	Polyacrylonitrile
PBO	Poly(p-phenylene benzobisoxazole)
PE	Polyethylene
PET	Poly(p-ethylene terephthalate)
PIPD	Poly({2,6-diimidazole[4,5-*b*:4′,5′-*e*]pyridinylene-1,4(2,5-dihydroxy)phenylene})
POK	Polyetherketone
PpPTA	Poly(p-phenylene terephthalamide)
$P(\sigma)$	Cumulative failure probability
$\langle P_2 \rangle$	Internal order parameter
P_D	Order parameter of the directors
q	Crack size
r	Radius of chain cross section
RH	Relative humidity
s.s.	Spinning speed
t	Time
t_b	Lifetime
T	Temperature
T_g	Glass transition temperature
T_{ni}	Nematic–isotropic transition temperature
T_0	Reference or Vogel temperature
u	Chain length
u_a	Average chain length
u_c	Bonded chain length
u_0	Monomer length
U	Activation energy
UHMW	Ultra-high molecular weight
V	Volume
V_c	Chain volume fraction
V_{cell}	Unit cell volume
W	Strain energy
W_a	Activation energy of creep
W_b	Fracture energy
W^C	Strain energy of the chain
W^S	Shear energy

W_m^S	Maximum shear energy
W_0^S	Shear energy of fracture
w_γ	Surface energy of a crack
z	Chain length in monomeric units
z_c	Bonded chain length in m.u.
z_n	Number-average chain length in m.u.
z_w	Weight-average chain length in m.u.

Greek symbols

β	Critical shear strain in tensor notation
γ	Shear strain in engineering notation
δ	Relaxation time
ε	Strain
ε_b	Strain at fracture
ε_b^s	Shear strain at fracture
ε_f	Fibre strain
ε_0	Ultimate strain at fracture
ε_f^y	Yield strain of the fibre
ε_{13}	Shear strain in tensor notation
ε_{13}^v	Viscoelastic shear strain of a domain
ε_{13}^y	Shear yield strain in tensor notation
ζ	Strength of orienting nematic potential
η	Viscosity
θ	Orientation angle at stress σ
θ_b	Orientation angle at fracture
Θ	Orientation angle in the unloaded state
λ	Load rate
ν	Frequency
$\rho(\theta)$	Orientation distribution of the chains
σ	Stress
σ_b	Tensile strength
σ_b^s	Fibre strength based on shear deformation only
σ_{comp}	Strength of a macrocomposite
σ_0	Ultimate strength
σ_L	Longitudinal strength
σ_T	Transverse strength
σ_y	Yield stress
τ	Shear stress
τ_b	Shear strength
τ_m	Maximum shear stress
τ_n	Normalised shear stress
τ_y	Shear yield stress
τ_0	Ultimate shear strength
χ	Euler's constant
ω	Angular frequency
Ω	Activation volume

1 Introduction

Organic polymer fibres offer an impressive range of mechanical properties. The tensile modulus of these fibres varies between 5 and 330 GPa, with a tensile strength up to 7 GPa, a compressive strength up to 1.7 GPa, and a temperature resistance up to 400 °C. The tensile curves of these fibres for temperatures below the glass transition temperature, including the yield phenomenon, are well described by the continuous chain model [1–10]. Considerable attention has been given in the literature to the relation between the tensile strength and the chain length distribution [11–14]. As will be shown here, there are also other factors of similar importance which determine the strength of a polymer fibre. In this report a relationship is derived describing the fibre strength as a function of the orientation distribution of the chains and the intrinsic mechanical properties, such as the elastic modulus of the polymer chain and the modulus for shear between the chains. In addition, a modified version of Yoon's model for the description of the relation between the strength and the chain length distribution is presented. Finally, a model is proposed for the dependence of the fibre strength on the time and the temperature.

Before embarking on the discussion of these intrinsic factors determining the strength of polymer fibres, the effect of structural and morphological imperfections on the fibre strength are briefly discussed. During the manufacturing process of polymer fibres all kinds of imperfections are introduced, like structural inhomogeneities, impurities and voids. These so-called extrinsic factors result in an imperfect bonding between the chains and may give rise to stress concentrations, which after a catastrophic growth of pre-existing cracks can lead to fracture. These imperfections cause the size effects, viz. the transverse effect or the dependence of the strength on the fibre diameter, and the longitudinal effect or the dependence of the strength on the test length [15–17]. Two different approaches can be recognised for the description of the size effects. The first is based on Griffith's theory of crack propagation, which considers the energy balance between the external work, the surface energy of the crack and the elastic energy of the material [18, 19]. This theory is based on the elastic theory of infinitesimal deformations, and so does not apply to highly deformable materials. It can be applied to the transverse effects and leads to the semi-empirical equation for the strength of a material

$$\frac{1}{\sigma_b} = \frac{1}{\sigma_0} + K \cdot \sqrt{D} \tag{1}$$

where σ_b is the actual strength of the fibre, σ_0 the strength of the flawless fibre or the ultimate strength, K a constant and D the diameter of the fibre [20]. It was later shown by Penning et al. that the scaling of the tensile strength with $D^{-0.5}$ can be derived from geometrical considerations as well [16]. An example of this relation is presented in Fig. 1, where the yarn strength of poly(*p*-phenyl-

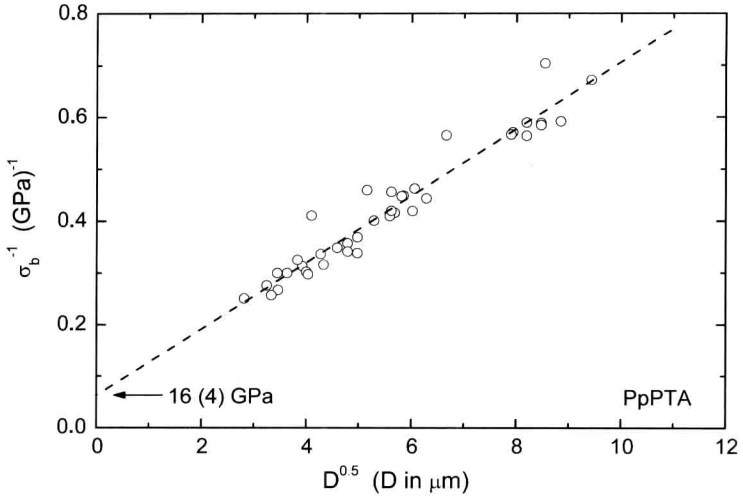

Fig. 1 The inverse of the observed strength of PpPTA yarns versus the square root of the diameter of the filaments. Linear regression yields σ_b^{-1}=0.063(16)+0.0643(27) $D^{0.5}$ (GPa)$^{-1}$ with σ_0=16(4) GPa, and estimated standard deviations in parentheses

ene terephthalamide) or PpPTA is plotted versus the filament diameter [21]. Apparently, for the strength of a flawless PpPTA filament the extrapolation yields σ_0=16±4 GPa. As will be shown in this report, this value is too large.

Whereas in the second approach of the size effects it is also assumed that fracture is controlled by defects, the strength is now considered a statistically distributed parameter rather than a physical property characterised by a single value. The statistical distribution of fibre strength is usually described by the Weibull model [22, 23]. In this weakest-link model the strength distribution of a series arrangement of units of length L_0 is given by

$$P(\sigma) = 1 - \exp\left[-\frac{L}{L_0}\left(\frac{\sigma}{\sigma_p}\right)^m\right] \tag{2}$$

where $P(\sigma)$ is the cumulative failure probability at a stress σ, σ_p a scaling parameter and m the Weibull modulus. To make a so-called Weibull plot of a yarn $P(\sigma)$ is approximated by

$$P = \frac{n_i}{n+1} \tag{3}$$

where n_i is the number of filaments that have broken at or below a stress σ and n is the total number of filaments tested. The length dependence is expressed through the test length L and can be written as

$$\log[-\log(1-P)] - \log L + \log L_0 = m\log\sigma - m\log\sigma_p \tag{4}$$

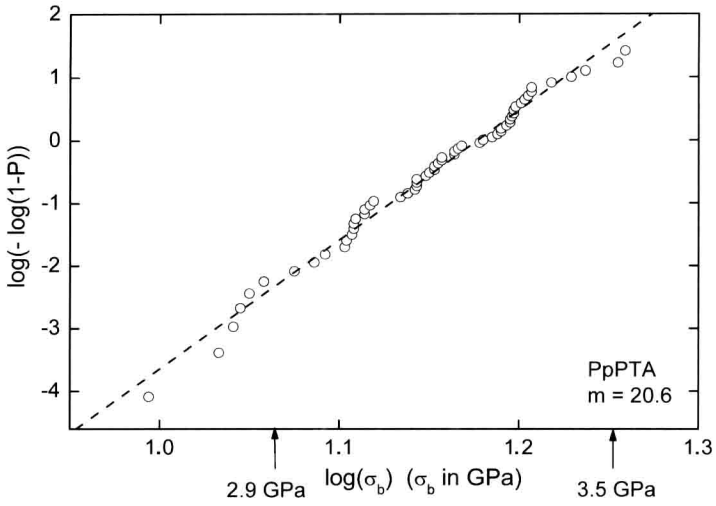

Fig. 2 Weibull plot of the filament strength for a test length of 10 cm of a PpPTA yarn yielding a Weibull modulus of 20.6. The average filament strength is 3.2 GPa

Thus, given a Weibull distribution of the filament strength, a plot of log [-log(1–*P*)] versus logσ results in a straight line with a slope *m*. For the range $5<m<30$ the relation between the coefficient of variance (cv) of the filament tenacity distribution and *m* is given by $cv=1.2\ m^{-1}$. Figure 2 presents an example of a Weibull plot of the filament strength of a PpPTA yarn, yielding a Weibull modulus of 20.6.

The average fracture stress of the filaments for a test length *L* is given by

$$\langle\sigma\rangle = \sigma_p L^{-\frac{1}{m}} \Gamma\left(1+\frac{1}{m}\right) \tag{5}$$

where Γ is the gamma function [15]. Equation 5 shows that the average strength depends on the test length of the fibre sample, which can be approximated by

$$\log(\langle\sigma\rangle) \approx C - \frac{1}{m}\log(L) \quad \text{with} \quad C = \log[\sigma_p \Gamma(1+1/m)] \tag{6}$$

Thus, the Weibull modulus can be derived from the strength distribution at a fixed test length as shown by Eq. 4, as well as from a plot of the average filament strength as a function of the test length according to Eq. 6. In Fig. 3, an example of the relation in Eq. 6 is presented for a PAN-based carbon fibre [8]. From this plot a value $m=7.2$ with an estimated standard deviation (esd) of 0.7 is derived, whereas the *m* values obtained from the strength distributions at fixed length are 5.2 (0.6) for 2 mm, 5.1 (0.6) for 10 mm and 4.6 (0.6) for 25 mm, with esd values in parentheses. Apparently the length effect is weaker than expected

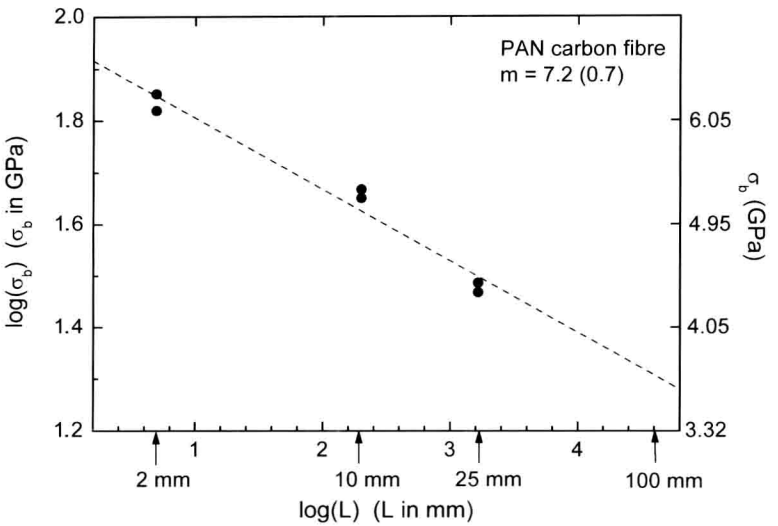

Fig. 3 The natural logarithm of the average filament strength (n=40) as a function of the natural logarithm of the test length for an intermediate-modulus, PAN-based carbon fibre with an impregnated bundle strength of 5.7 GPa [8]

from the width of the strength distributions at fixed length, which may indicate that adjacent segments in the carbon filament are not statistically independent, as is assumed by the weakest-link theory, i.e. the model is not quite suitable. With regard to the application of fibres in uniaxially reinforced composites, the critical length of a fibre is the test length for which the average filament tenacity is equal to the impregnated bundle strength. Since the impregnated bundle strength of this carbon fibre is 5.7 GPa, it follows from Fig. 3 that the critical length is 4.5 mm. Weibull moduli of filaments taken from yarns range from 5 for brittle carbon fibres to about 50 for ductile melt-spun poly(p-ethylene terephthalate) (PET) fibres.

Penning et al. studied the transverse and longitudinal size effects in high-strength ultra-high molecular weight (UHMW) polyethylene (PE) fibres and found that the length or longitudinal size effects become weaker as the tensile modulus of the fibre increases, whereas the transverse effect becomes more pronounced as the modulus increases [16]. In particular, the length effect disappeared almost completely for PE fibres with a draw ratio of 70. This was attributed by Penning et al. to the fact that the high-modulus PE fibres do not possess a distribution of macroscopic flaws, occurring at distances of the same order of magnitude as the applied test lengths, but contain a microscopic defect structure at very short intervals of about 100 nm. They concluded that, apparently, transverse and longitudinal effects have different physical backgrounds and, therefore, cannot be described simultaneously by statistical theories such as the weakest-link hypothesis. In the case of high-modulus/high-strength

fibres, such as PpPTA and poly(*p*-phenylene benzobisoxazole) or PBO, and poly({2,6-diimidazole[4,5-*b*:4′,5′-*e*]pyridinylene-1,4(2,5-dihydroxy)phenylene}) or PIPD, made by the wet-spinning process, the transverse size effect is difficult to detect, because a decrease of the filament diameter is often accompanied by an increase of the tensile modulus. As will be shown in Sect. 2 this results in an increase of the strength. In this regard the conclusions drawn from Fig. 1 should be considered with some caution. With regard to the observation of Penning at el. that the longitudinal size effect becomes weaker as the modulus increases, it will be shown in this report that, by applying Griffith's theory on cracks in anisotropic fibres, elongated cracks are supposed to be more damaging in low-oriented fibres than in highly oriented fibres.

An extensive discussion of the concept of fibre strength, the Weibull modulus, and its relation to fracture toughness has been given by Van der Zwaag [15]. An increase of the material toughness will result in an increase of the Weibull modulus, because incorporation of local plastic deformation will decrease the stress concentrations in the fibre. This is much more easily achieved with flexible polymer chains than with rigid-rod chains, not to mention the graphitic planes in carbon fibres. Van der Waals and hydrogen bonds offer more advantages in this respect than covalent bonds between the building elements of the fibre. This explains the observation that the Weibull modulus of yarns decreases according to the sequence: PE, PET, cellulose, PpPTA, PBO and carbon fibre. The particularly low value of the Weibull modulus of carbon fibres is a consequence of the brittleness of these fibres. Therefore, the increase of the strength of carbon fibres calls for extreme care at each stage of the process to preclude any kind of flaw-producing impurity [24].

Melt-spun fibres such as PET displaying a "flag" or a plastic mode of deformation at the end of the tensile curve show a large variation of the elongation at break. At low tensile speeds these fibres display ductile fracture initiated by crack growth, and for increasing testing speeds the melt fracture morphology becomes dominant. Adiabatic heating of the fibre during rapid cold drawing will raise the temperature well above the glass transition temperature [25]. But even at medium strain rates of 100% per minute tiny irregularities in the fibre may cause localised drawing or "necking", whereby the temperature can approach the melting temperature, resulting in an extra elongation before fracture. Hence, this random phenomenon of "hot spots" occurring during cold drawing causes the wide range of elongations at break observed during filament testing of PET fibres. With regard to the failure mode, it is significant to note that polymer fibres without a melting temperature, such as cellulose, PpPTA, PBO and PIPD, generally display a more or less fibrillar fracture morphology. This is in contrast to polymer fibres having a melting temperature like PE, PET and the aliphatic polyamides, which often show melt-flow phenomena during cold drawing.

Weibull plots of various fibre properties, such as the filament count, modulus, elongation at break and the strength, can provide important information on the quality and performance of the manufacturing process. The results can be used to formulate a strategy for the improvement of the yarn properties.

As will be shown in this report, polymer fibres gain additional strength by an increase of the molecular weight and by a more contracted orientation distribution, i.e. a higher modulus. For the wet-spun fibres, a strength increase can be achieved by improvement of the coagulation process, which makes for a more uniform structure and chain orientation in the cross section of the fibre, and by a reduction of the amount of impurities.

For an understanding of the fracture process and the dependence of the strength on the chain orientation distribution and the basic elastic constants, we briefly discuss the tensile deformation of polymer fibres. The continuous chain model provides a good description of the tensile curve of a polymer fibre [1–10]. In this model the fibre is built up of parallel oriented fibrils with equal properties. Thus it is assumed that a mechanical model of the extension of a single fibril as a function of the fibre stress gives a complete description of the tensile deformation of the fibre. Each fibril is a series arrangement of domains consisting of perfectly oriented chains. The domains are cylindrically symmetric around the chain axis and the axes of the domains follow an orientation distribution, $\rho(\Theta)$, in the unloaded state. The elastic constants of the domain most relevant to the tensile extension of the fibre are the chain modulus, e_c, and the modulus for shear between adjacent chains, g. Figure 4 shows the stresses acting on a domain due to a tensile stress on the fibre and Figs. 5 and 6 depict schematic representations of the domain deformation according to the continuous chain model. The fibre strain is given by

$$\varepsilon_f = \frac{\sigma\langle\cos^2\theta\rangle}{e_c} + \frac{\langle\cos\theta\rangle - \langle\cos\Theta\rangle}{\langle\cos\Theta\rangle} \tag{7}$$

where Θ is the initial orientation angle of the chain axis at zero load and θ the angle at a tensile stress σ. The averaging is performed over the chain orientation distributions $\rho(\Theta)$ and $\rho(\theta)$ of the domains in the fibril. As shown by Eq. 7 the fibre strain is composed of two contributions, viz. the elastic chain exten-

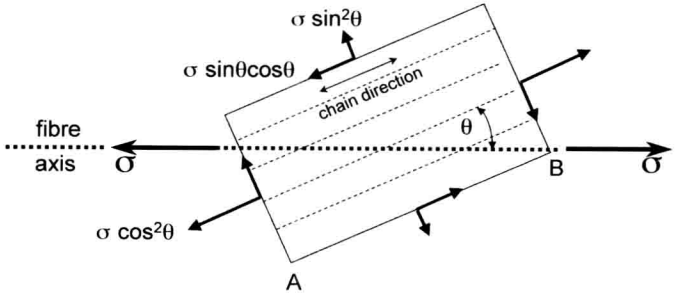

Fig. 4 The four normal stresses and the four equal shear stresses acting on the domain in the fibre under a tensile stress σ. The chains are parallel to AB and make an angle θ with the fibre axis